

Control method of high-speed switched reluctance motor with an asymmetric rotor magnetic circuit

PIOTR BOGUSZ, MARIUSZ KORKOSZ, JAN PROKOP

*Rzeszow University of Technology
Faculty of Electrical and Computer Engineering
ul. Wincentego Pola 2, 35-959 Rzeszów, Poland
e-mail: pbogu/mkosz/jprokop@prz.edu.pl*

(Received: 12.11.2015, revised: 29.08.2016)

Abstract: In the paper, the modified (compared to the classical asymmetric half-bridge) converter for a switched reluctance machine with an asymmetric rotor magnetic circuit was analysed. An analysis for two various structures of switched reluctance motors was conducted. The rotor shaping was used to obtain required start-up torque or/and to obtain less electromagnetic torque ripple. The discussed converter gives a possibility to turn a phase off much later while reduced time of a current flows in a negative slope of inductance. The results of the research in the form of waveforms of currents, voltages and electromagnetic torque were presented. Conclusions were formulated concerning the comparison of the characteristics of SRM supplied by the classic converter and by the one supplied by the analysed converter.

Key words: switched reluctance motor, SRM, power converter, electromagnetic torque

1. Introduction

Switched reluctance machines are categorized among machines with electronic commutation [1-2] i.e. they require a power electronic converter for proper operation. A proper control algorithm is also required. A turn-off angle in a SRM is linked with the so called aligned position of a rotor for each phase. However, in practice this is possible only at speed close to zero. By increasing speed, it is required to turn each phase off much earlier. It is connected with the current which flows in a negative slope of inductance and hence the motor produces a negative electromagnetic torque. A delayed turn off causes not only a decrease of average torque but also an increase of torque ripple and decrease of an efficiency of the machine. This problem concerns structures where there is a deliberate deformation of rotor magnetic circuit to obtain a required value of a start-up torque [2]. The deliberate deformation of a rotor magnetic circuit can also be used to limit ripple of the generated electromagnetic torque [2-4].

In this paper, the modified C-dump converter which allows an extension of a conduction angle was analysed. The analysed circuit allows also faster discharge of accumulated energy in motor windings than in the classic asymmetric half-bridge. Sample waveforms of currents,

voltages and electromagnetic torque of the motor supplied by the analysed converter and the classic asymmetric half-bridge were presented.

2. Overview of converter topologies, problem description

Several varieties of SRM converter topologies have been already presented the literature of the subject [1-2, 5-8]. Fig. 1a shows one branch of the classic asymmetric half-bridge.

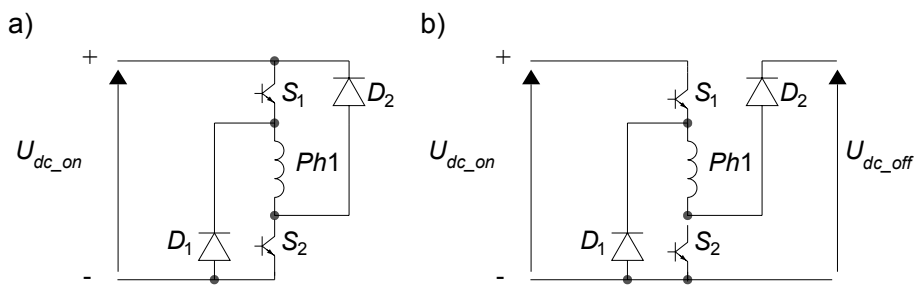


Fig. 1. The classic asymmetric half-bridge (a) and the half-bridge with separated voltages U_{dc_on} and U_{dc_off} (b)

After turning on both switches S_1 and S_2 , the supply voltage U_{dc} is applied to the phase and after turning them off stored energy in the magnetic field is returned to the supply source through the diodes D_1 and D_2 . A time when both switches S_1 and S_2 are turned off is connected with working conditions of a motor. When speed is increasing, it is crucial to take into account a sufficient time period to discharge all the stored energy in the magnetic field. A delayed turn off leads to a generation of a negative value of electromagnetic torque, which in consequence leads to an increase of electromagnetic torque ripple and a decrease of average electromagnetic torque. Fig. 1b shows the unipolar half-bridge, where two voltages U_{dc_on} and U_{dc_off} were separated [5]. In this case, after turning on both switches S_1 and S_2 , U_{dc_on} is applied to the phase. After turning them off, U_{dc_off} is applied to the phase and in consequence the phase returns energy to the supply source. If $U_{dc_off} > U_{dc_on}$ then discharging time of stored energy is shorter. Figs. 2-4 show sample waveforms of the phase voltage u_{ph} (Fig. 2a), the phase current i_{ph} (Fig. 2b) and the electromagnetic torque T_e (Fig. 2c) for converters from Figs. 1a-b. In the circuit from Fig. 1b, an assumption that $U_{dc_off} = kU_{dc_on}$ was made (where $k > 1$).

There are at least several types of power converters with two values of a voltage i.e. where $U_{dc_off} > U_{dc_on}$. Fig. 3 shows three power converter topologies which meet the above mentioned condition [2, 7, 8].

Fig. 3a shows a topology of a converter where there is a possibility to regulate a supply voltage by an additional circuit made of elements S_d , L_d , D_d . Such a solution eliminates the necessity to PWM control of transistors S_1 and S_2 in a phase circuit. The value of the U_{dc_off} voltage is forced by the supply voltage U_{dc} . Fig. 3b shows the second converter topology which meets the condition $U_{dc_off} > U_{dc_on}$.

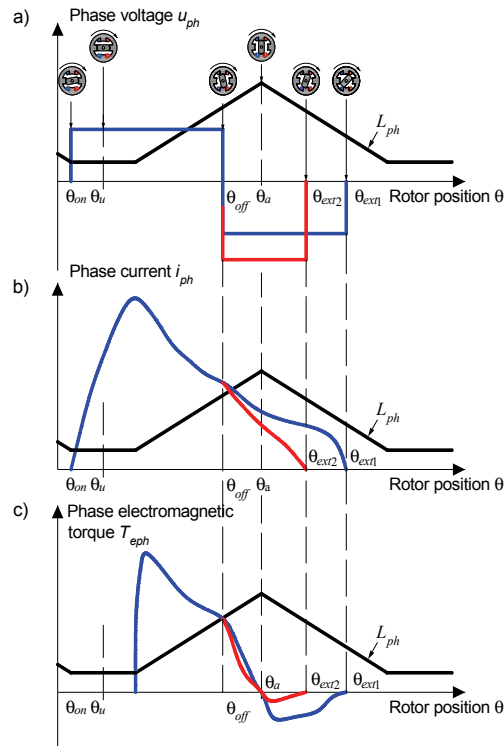


Fig. 2. Theoretical waveforms of a) phase voltages u_{ph} , b) phase current, c) phase electromagnetic torque for circuits from Figs. 1a (blue line) and 1b (red line)

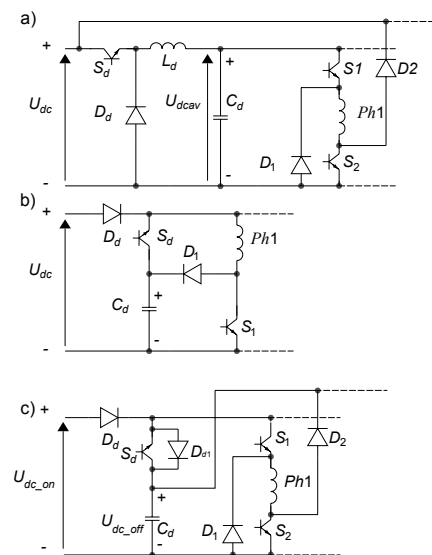


Fig. 3. The classic unipolar half-bridge with regulation of average value of U_{dc_on} (a), the C-dump converter with a zero-volt loop (b), modified C-dump converter (c)

The main feature of this circuit is a possibility to PWM control with a zero-volt state and fast decreasing of a current because U_{dc_off} is higher than U_{dc_on} . A higher value of U_{dc_off} appears as a result of energy reloading from the winding which is turned off to the capacitor C_d . When phase currents start to overlap each other then turning the transistor S_d on causes a significant extension of a decreasing time of a phase current in an outgoing phase. This is a drawback of this converter.

Fig. 3c shows the converter which allows much faster discharge of accumulated energy in the magnetic field of the machine [8]. The converter was marked as “H + 1”, but in the literature it was called as “modified C-dump converter”. In the converter, an additional switch S_1 and a diode D_1 was used in comparison to the converter from Fig. 3b. By using the switch S_1 and the diode D_1 , it is possible to turn a switch S_d off at any time without increasing a falling time of the phase current but decreasing it when the switch S_1 is turned off. The analysed converter also allows the generation of a zero-volt state.

The energy flow changes in the circuit according to the combination of the switches' states (turned on or turned off). In the analysed converter, particular operation modes of the circuit are possible:

- The switches S_1 and S_2 are turned on and the switch S_d is turned off. In this mode, the winding is supplied with U_{dc_on} voltage.
- The switches S_1 , S_2 and S_d are turned on. The winding is supplied with U_{dc_off} when voltage of a capacitor C_d is greater than U_{dc_on} , otherwise the winding is supplied with U_{dc_on} .
- The switch S_1 is turned off, the switch S_2 is turned on and the switch S_d can be turned on or turned off, because the winding is in a zero-volt state.
- The switch S_1 is turned on and the switches S_2 and S_d are both turned off – energy from the winding is recharged to the capacitor C_d through the diode D_2 .
- The switch S_2 is turned off and the switches S_d and S_1 are both turned on. The winding is in a zero-volt state and the current flows through the winding, the diode D_2 and the switches S_1 and S_d .

These are not the only converters which meet the condition $U_{dc_off} > U_{dc_on}$. Such type also includes the ACRDEL converter [5] or the converter with two supply sources [6]. This situation where $U_{dc_off} > U_{dc}$ occurs also in circuits analysed in papers [9-14]. Reduction of energy return time can be also achieved in multilevel circuits [15-16].

3. Analysed structures of two-phase switched reluctance motors

The converter from Fig. 3c was applied when studies on a switched reluctance motor designated for high-speed drives of household appliances (two-phase with $U_{dc} = 310$ V, $P_N = 700$ W, $n_N = 45000$ r/min) were conducted. A structure of a motor with an asymmetric step-air gap to obtain desired start-up torque was one of the studied versions of a rotor shape. Alternatively, the solution with reduced stator pole-arc and with a dual step-air gap was also proposed [17]. Both analysed structures are shown in Fig. 4.

In the classic solution shown in Figs. 4a, 4c, the intentional deformation of the rotor was made to obtain sufficient value of start-up torque in any rotor position. In the alternative solution shown in Figs. 4b, 4d, the deformation of the rotor was made to limit electromagnetic torque ripple.

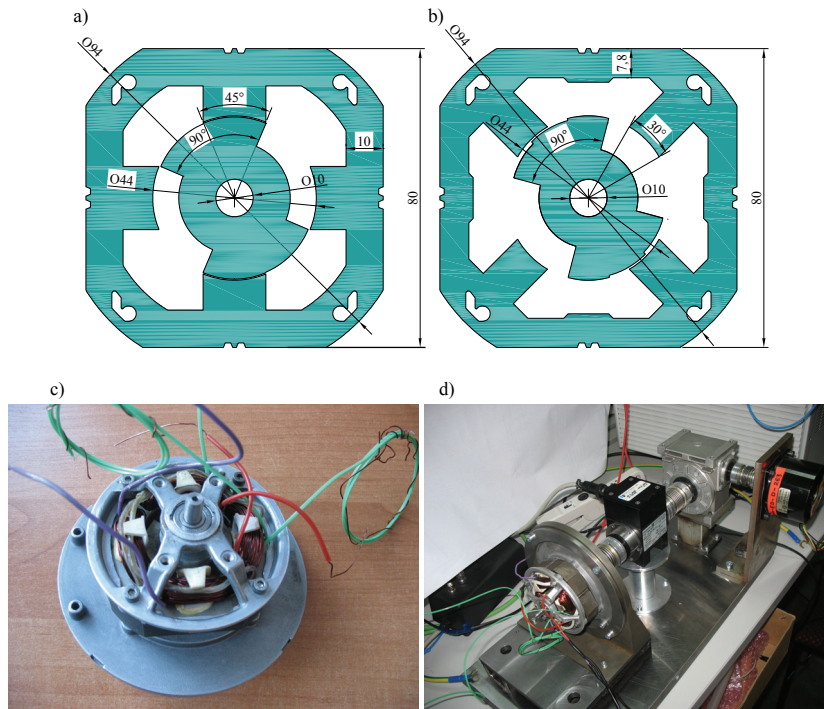


Fig. 4. Structures of two-phase switched reluctance motors a) stator and rotor geometry of the classic structure with a pole-arc $\beta_s = 45^\circ$ and a step-air gap, b) stator and rotor geometry of the alternative structure with a stator pole-arc $\beta_s = 30^\circ$ and a dual step-air gap, c) motor prototype of the classic structure with a pole-arc $\beta_s = 45^\circ$ and a step-air gap, d) the laboratory setup used to determine static characteristics

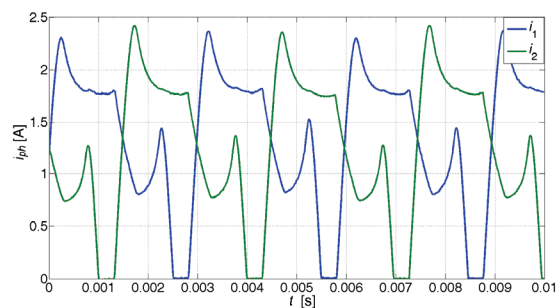


Fig. 5. Waveforms of phase currents of the two-phase switched reluctance motor with an asymmetric rotor

Both solutions have advantages (a possibility to start the motor from any rotor position) and disadvantages (a high sensitivity to changes of a turn-off angle). A delayed phase turn-off causes that the current flows in a negative slope of inductance. In a negative slope of inductance, the induced voltage has a significantly higher value which can lead to an increase of the phase current. Fig. 5 shows the sample waveforms of phase currents of 4/2 SRM registered for the structure of the motor from Fig. 4b. Motor currents were registered at a relatively high value of a turn-off angle at $n = 10000$ r/min with no-load ($U_{dc} = 50$ V, $\theta_{on} = 0^\circ$, $\theta_{off} = 90^\circ$).

Figs. 6-7 show dependencies of self-inductances L_{ph} of motor phases determined by the bridge method [17-18].

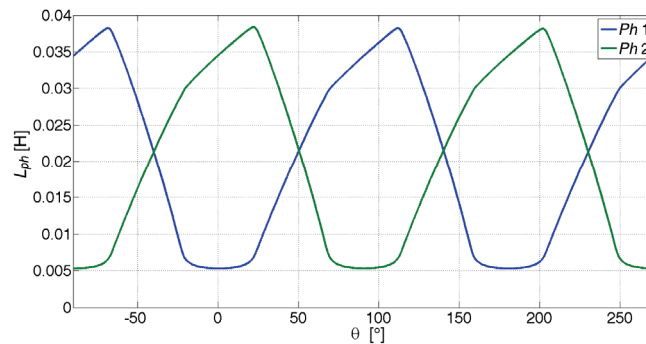


Fig. 6. A dependence of the self-inductance L_{ph} in the function of the rotor position θ of the two-phase SRM from Fig. 4a

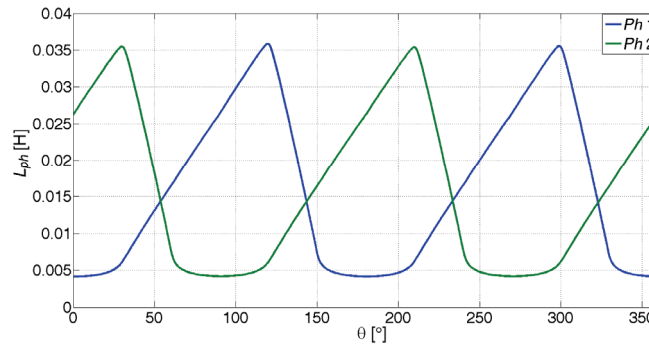


Fig. 7. A dependence of the self-inductance L_{ph} in the function of the rotor position θ of the two-phase SRM from Fig. 4b

Figs. 8-9 show sample static characteristics of two-phase 4/2 switched reluctance motors shown in Fig. 4 [17-18]. Characteristics were determined in laboratory conditions for various values of a phase current. As it can be observed, a flow of the phase current above angle 110° (for the structure from Fig. 4a) or 120° (for the structure from Fig. 4b) causes a generation of a negative electromagnetic torque.

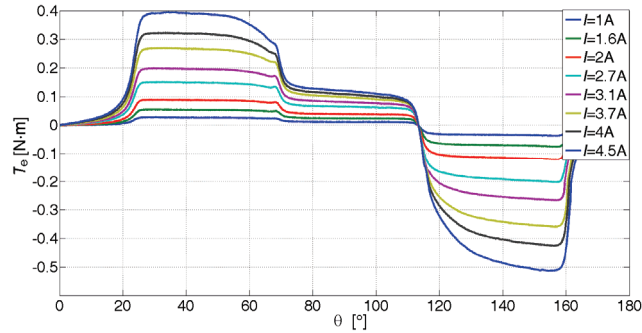


Fig. 8. A dependence of the torque T_e in the function of the rotor position θ at $I = \text{var}$ of the two-phase SRM from Fig. 4a

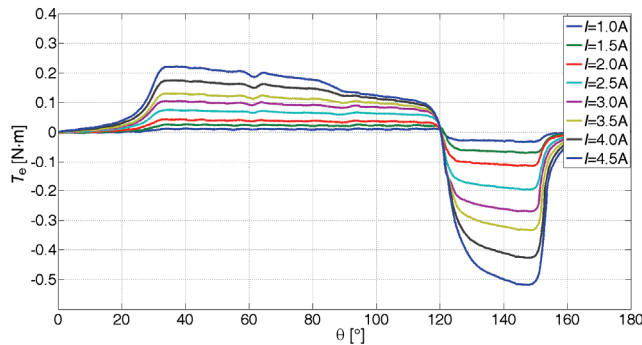


Fig. 9. A dependence of the torque T_e in the function of the rotor position θ at $I = \text{var}$ of the two-phase SRM from Fig. 4b

Both structures were designed to obtain initial start-up torque being not less than 0.09 Nm at winding current $I = 4$ A. The structure from Fig. 4b was designed to obtain flatter torque characteristic and it was obtained by introduction an additional air gap. Flat torque characteristic makes that electromagnetic torque ripples are limited in the two-phase structure. The structure from Fig. 4b has a reduced stator pole-arc to 30° , in contrast with 45° for the structure from Fig. 4a. The same value of a negative torque occurs in both structures at the same winding current. In a high-speed drive, during motoring operation, current flow during descending part of inductance (Figs. 6-7) is connected with generation of braking torque. To avoid this problem, it is required to turn phases off earlier or discharge accumulated energy faster in windings. The measurement results in Figs. 6-9 were prepared in Matlab environment [19].

4. Analysed supply method of the two-phase SRM

By using the described circuit from Fig. 3c to supply two-phase 4/2 SRM with a rotor with a step-air gap, it is possible to reduce a falling time of the current in the outgoing phase by

proper control of circuit switches despite a wide conduction period. It was assumed that the initial voltage on the capacitor U_{dc_off} is higher than the supply voltage U_{dc_on} . Fig. 10 shows typical operation modes of the H+1 converter connected with energy flow.

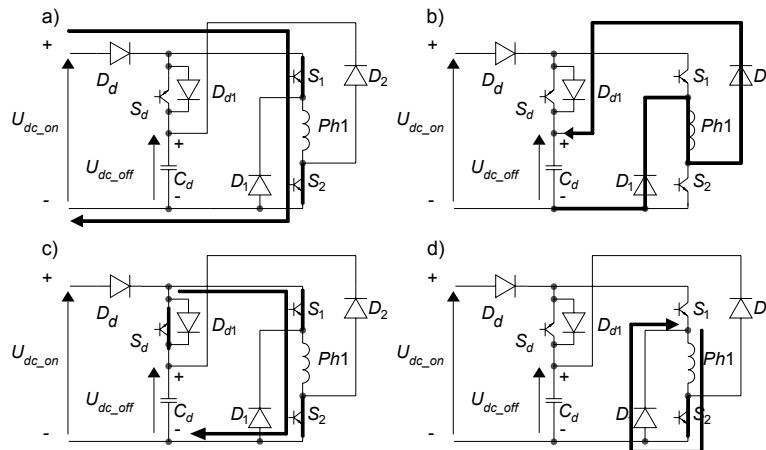


Fig. 10. Typical operation modes of the H+1 converter: supply with the voltage U_{dc_on} (a), energy return with an initial condition $U_{dc_off} = U_{dc_on}$ (b), discharging of the capacitor C_d (c), a zero-volt state (d)

Fig. 10a shows the state when the winding is supplied with U_{dc_on} (switches S_1 and S_2 on and switch S_d off). After turning on switch S_d (Fig. 10c) the winding is supplied with U_{dc_off} which is higher than U_{dc_on} . An instant of turning on switch S_d should be chosen to ensure that accumulated energy in the capacitor C_d is completely discharged before turning switches S_1 and S_2 off. It is possible to turn the winding off (switches S_1 and S_2 off) when switch S_d is turned off (Fig. 10b). Diode D_{d1} ensures that a condition $U_{dc_off} = U_{dc_on}$ is met when switch S_d is turned off earlier. When the capacitor C_d is completely discharged, the voltage at the beginning of discharging process of accumulated energy is $U_{dc_off} = U_{dc_on}$. The return of the energy to the capacitor C_d causes fast increase of the voltage U_{dc_off} , which in consequence leads to a significant reduction of a discharging time of accumulated energy in the magnetic field. This converter allows operation in the zero-volt state (Fig. 10d) and this state does not depend on a state of switch S_d .

When $U_{dc_off} > U_{dc_on}$ then accumulated energy in windings is discharged faster, but on the other hand a higher value of the voltage causes an increase in vibroacoustics of a motor. Due to the faster decrease of the phase current, the mechanical tension of stator magnetic circuit also decreases faster. A violent change of magnetic circuit tension causes an increase of the vibroacoustics level [2].

5. Mathematical and simulation model

The studies of the analysed power converter were conducted with a simulation model built on the basis of a mathematical model of the SRM. The model assumed negligibility of eddy currents in stator and rotor cores. Assuming that in the case of nonlinearity of the magnetic

circuit, the vector of flux-linkages $\boldsymbol{\psi}(\boldsymbol{\theta}, \boldsymbol{i})$ depends on a rotor position $\boldsymbol{\theta}$ and N phase currents i_1, \dots, i_N from the definitions as in [20]:

$$\boldsymbol{\psi}(\boldsymbol{\theta}, \boldsymbol{i}) = [\psi_1(\boldsymbol{\theta}, i_1, \dots, i_N), \dots, \psi_N(\boldsymbol{\theta}, i_1, \dots, i_N)]^T \quad (1)$$

equations of N – phase machine have the following structure:

$$\boldsymbol{u} = \boldsymbol{R}\boldsymbol{i} + \frac{d}{dt}\boldsymbol{\psi}(\boldsymbol{\theta}, \boldsymbol{i}), \quad (2)$$

$$J \frac{d\omega}{dt} + D\omega + T_L = T_e(\boldsymbol{\theta}, \boldsymbol{i}), \quad (3)$$

$$T_e(\boldsymbol{\theta}, \boldsymbol{i}) = \frac{\partial W_c^*(\boldsymbol{\theta}, \boldsymbol{i})}{\partial \boldsymbol{\theta}}, \quad (4)$$

where vectors of voltages \boldsymbol{u} , currents \boldsymbol{i} and the matrix of phase resistances \boldsymbol{R} are defined as: $\boldsymbol{u} = [u_1, \dots, u_N]^T$, $\boldsymbol{i} = [i_1, \dots, i_N]^T$, $\boldsymbol{R} = \text{diag}(R_1, \dots, R_N)$.

Moreover, the following symbols are used in Equations (1)-(4): $\boldsymbol{\theta}$ – the rotor position; J – the moment of inertia of a rotor; D – the coefficient of viscous friction; T_L – the load torque; $\omega = d\boldsymbol{\theta}/dt$ – the angular velocity of a rotor; T_e – the electromagnetic torque; and $W_c^*(\boldsymbol{\theta}, \boldsymbol{i})$ – the magnetic field co-energy in the machine's air gap.

Assuming that fluxes of individual phases $\boldsymbol{\psi}_1, \dots, \boldsymbol{\psi}_N$ can be expressed as a sum of fluxes, each depending on only one phase current, according to the definition:

$$\boldsymbol{\psi}(\boldsymbol{\theta}, \boldsymbol{i}) = \left[\sum_{j=1}^N \boldsymbol{\psi}_{1j}(\boldsymbol{\theta}, i_j), \dots, \sum_{j=1}^N \boldsymbol{\psi}_{Nj}(\boldsymbol{\theta}, i_j) \right]^T, \quad (5)$$

the electromagnetic torque T_e of N -phase switched reluctance machine (4) can be expressed as in [17, 19]:

$$T_e(\boldsymbol{\theta}, i_1, \dots, i_N) = \sum_{i=1}^N \sum_{j=1}^i \frac{\partial}{\partial \boldsymbol{\theta}} \int_0^{i_j} \boldsymbol{\psi}_{ij}(\boldsymbol{\theta}, i_j) di_j. \quad (6)$$

To build a simulation model, it is assumed that the vector of flux-linkages (5) can be written as:

$$\boldsymbol{\psi}(\boldsymbol{\theta}, \boldsymbol{i}) = \boldsymbol{\psi}_{\text{self}}(\boldsymbol{\theta}, \boldsymbol{i}) + \boldsymbol{\psi}_{\text{mutual}}(\boldsymbol{\theta}, \boldsymbol{i}), \quad (7)$$

where vectors of the self-inductance and the mutual inductance are defined as:

$$\boldsymbol{\psi}_{\text{self}}(\boldsymbol{\theta}, \boldsymbol{i}) = [\psi_{11}(\boldsymbol{\theta}, i_1), \dots, \psi_{NN}(\boldsymbol{\theta}, i_N)]^T \quad (8)$$

$$\Psi_{\text{mutual}}(\theta, \mathbf{i}) = \left[\sum_{j=2}^N \Psi_{1j}(\theta, i_j) \quad \dots \quad \sum_{j=1}^{N-1} \Psi_{Nj}(\theta, i_j) \right]^T \quad (9)$$

Figure 13 shows a block diagram of the SRM simulation model based on voltage-current Equation (2) with mutual couplings between phases taken into account (Fig. 11a) and a block diagram of the torque Equation (3) (Fig. 11b).

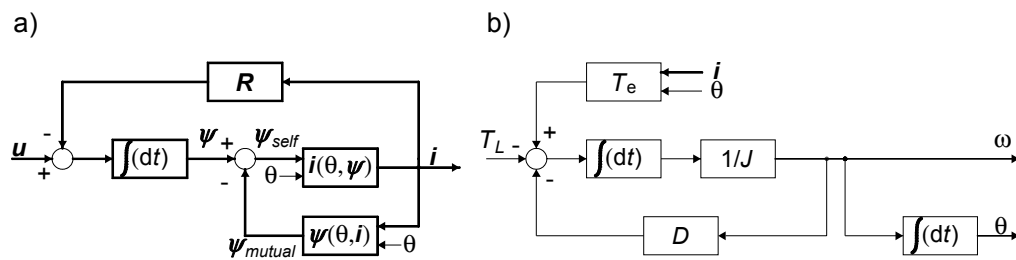


Fig. 11. A block diagram representing voltage-current equations (a) and a block diagram representing the torque equation (b) of the SRM simulation model

As it can be seen in Fig. 11a, it is necessary to determine inverse characteristics, i.e. relationships between individual phase current and its flux. The relationships based on the assumption of one-to-one correspondence of the involved quantities, can be represented by the certain function $f(\cdot)$ depending on the rotor position θ and the flux vector Ψ_{self} , i.e. it can be assumed that

$$\mathbf{i} = \mathbf{f}(\theta, \Psi_{\text{self}}) \quad (10)$$

Fig. 11b shows a block diagram depicting calculation of the electromagnetic torque according to (6). Block diagrams in Figs. 11a and 11b constitute a base to build a complete simulation model of the SRM which takes into account couplings between phases and allowing the analysis of static and dynamic states e.g. in the Matlab/Simulink environment [20].

6. Simulation results

Simulation studies were conducted to determine properties of the analysed converter marked as H + 1. Objects of studies were two-phase motors with an asymmetric magnetic circuit, which were shown in Fig. 3. Motors were designed to a high-speed drive with required rated speed $n_N = 45000$ r/min. Studies were conducted for two converters, the classic asymmetric half-bridge (Fig. 1a) and the H + 1 converter (Fig. 3c). The following conditions were assumed to compare both converters: $U_{dc} = 310$ V, $n_N = 45000$ r/min, $\theta_{on} = 0^\circ$, $\theta_{off} = 90^\circ$. The results of studies of the H-type converter with control parameters (marked as H*) selected to

obtain the same value of average electromagnetic torque T_{eav} as in the H + 1 converter were additionally placed.

6.1. The structure with a single step-air gap

In the structure with a single step-air gap, a value of a capacitance of the additional capacitor C_d was $1 \mu\text{F}$. Figs. 12-15 show the phase current i_{ph} (Fig. 12), the source current i_{dc} (Fig. 13), the phase voltage u_{ph} (Fig. 14) and the electromagnetic torque T_e (Fig. 15) in the function of the rotor position θ for both converters. A dependence of the flux-linkage ψ_1 with the phase $Ph1$ in the function of the current i_1 is shown in Fig. 16. Control angles were increased ($\theta_{\text{on}} = -10^\circ$ and $\theta_{\text{off}} = 80^\circ$) in the H-type converter to obtain the same value of average electromagnetic torque T_{eav} .

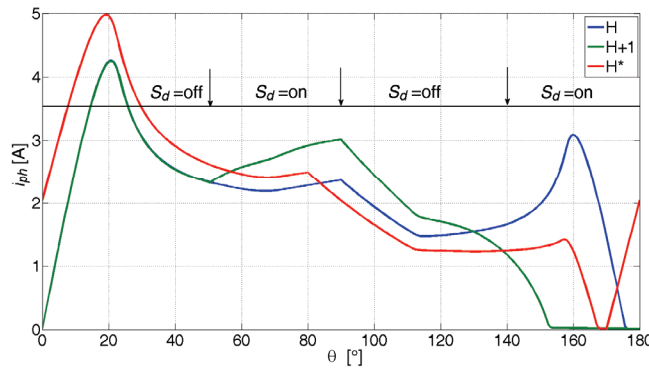


Fig. 12. A dependence of the phase current i_{ph} in the function of the rotor position θ for H and H + 1 converters

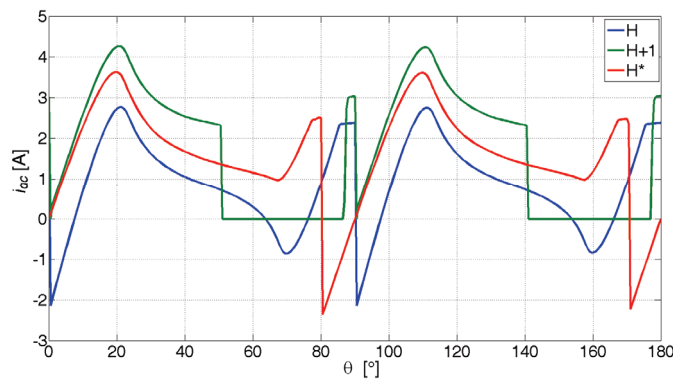


Fig. 13. A dependence of the source currents i_{dc} in the function of the rotor position θ for H and H + 1 converters

By using a classic H-type converter with the structure from Fig. 3a, it is not possible to turn phases off too late at high-speed operation. As it can be seen in Fig. 12, after turning phases off at $\theta_{\text{off}} = 90^\circ$, current can again increase because of change of back-emf sign.

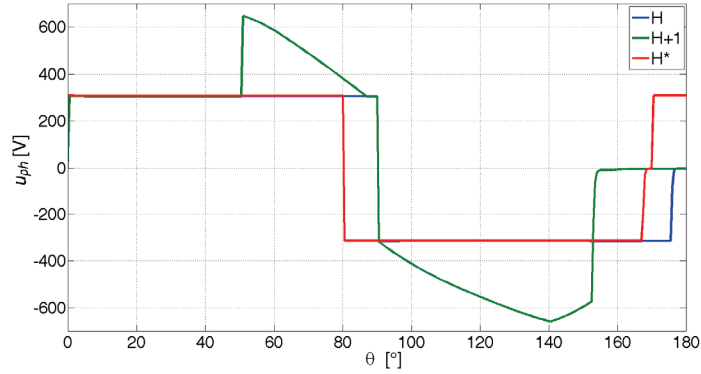


Fig. 14. A dependence of the phase voltage u_{ph} in the function of the rotor position θ for H and H + 1 converters

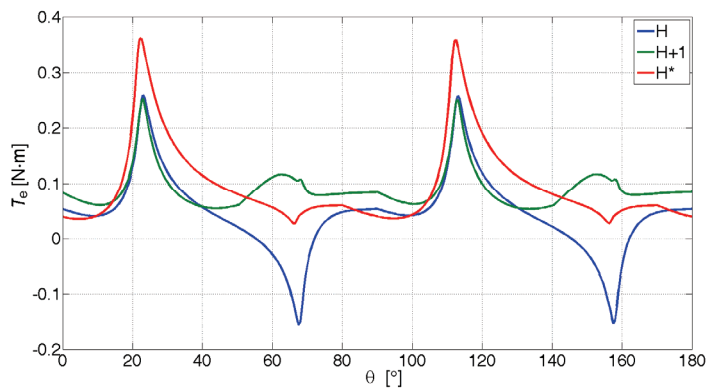


Fig. 15. A dependence of the electromagnetic torque T_e in the function of the rotor position θ for H and H + 1 converters

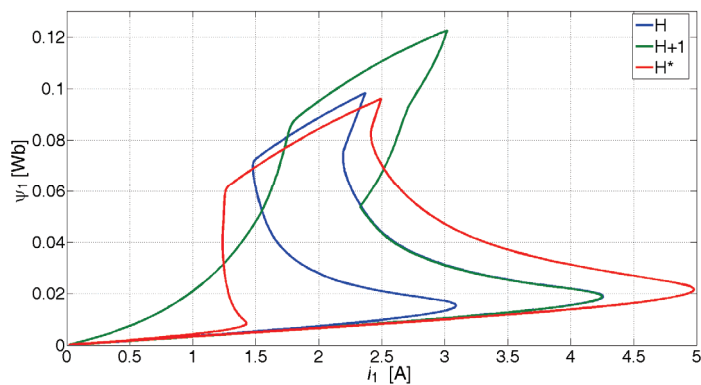


Fig. 16. A dependence of the flux-linkage ψ_l in the function of the phase current i_l for H and H + 1 converters

Therefore, high value of negative electromagnetic torque is generated (Fig. 15). It can be also seen in flux-linkage vs. phase current characteristics. The same supply conditions but with the H+1 converter lead to limited time of energy discharging of the phase. Consequently, electromagnetic torque ripples are also limited, although the structure from Fig. 6a was not designed to minimize torque ripple. So by using the classical H-type converter it is necessary to turn phases off earlier to avoid generation of braking torque T_e . Electromagnetic torque ripples are also limited but they are higher than in the H + 1 converter.

6.2. The structure with a dual step-air gap

In the structure with a dual step-air gap, a value of a capacitance of the additional capacitor C_d was 2 μ F. Figs. 17-20 show the phase current i_{ph} (Fig. 17), the source current i_{dc} (Fig. 18), the phase voltage u_{ph} (Fig. 19) and the electromagnetic torque T_e (Fig. 20) in the function of the rotor position θ for both converters. The dependence of the flux-linkage ψ_1 with the phase Ph1 in the function of the current i_1 is shown in Fig. 21. Control angles were increased ($\theta_{on} = -2.5^\circ$ and $\theta_{off} = 79.5^\circ$) in the H-type converter to obtain the same value of average electromagnetic torque T_{eav} .

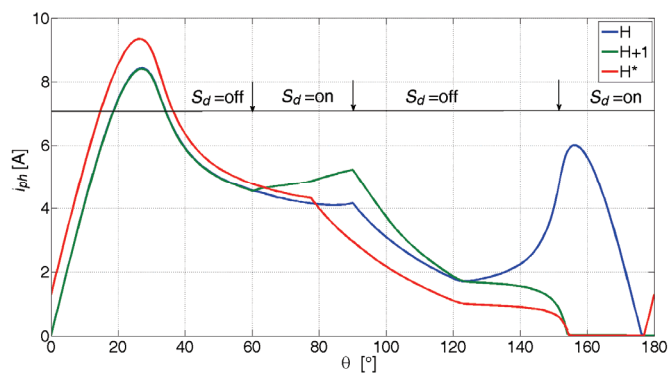


Fig. 17. A dependence of the phase current i_{ph} in the function of the rotor position θ for H and H + 1 converter

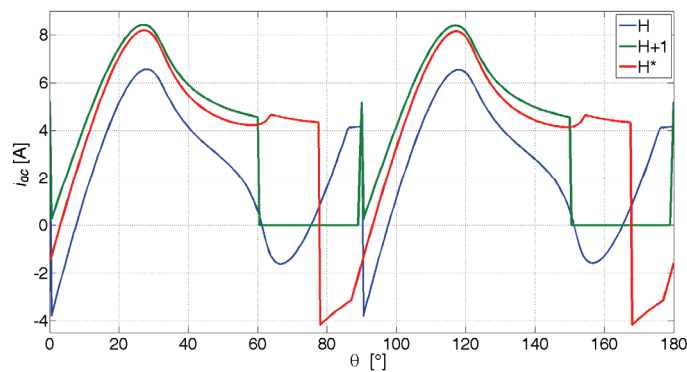


Fig. 18. A dependence of the source currents i_{dc} in the function of the rotor position θ for H and H + 1 converters

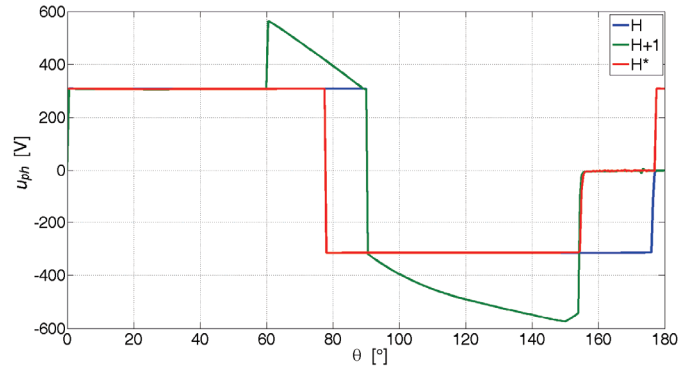


Fig. 19. A dependence of the phase voltage u_{ph} in the function of the rotor position θ for H and H + 1 converters

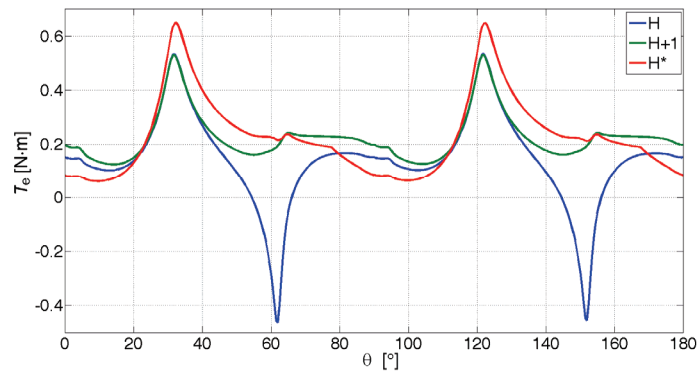


Fig. 20. A dependence of the electromagnetic torque T_e in the function of the rotor position θ for H and H + 1 converters

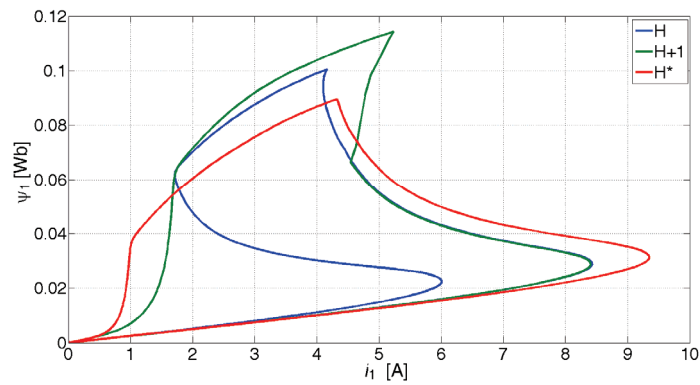


Fig. 21. A dependence of the flux-linkage ψ_1 in the function of the phase current i_1 for H and H + 1 converters

The structure from Fig. 3b was constructed to limit electromagnetic torque ripple, but it is highly sensitive to turn-on angle selection, simultaneously. A late turn of a phase off ($\theta_{off} = 90^\circ$) causes generation of a high value of negative electromagnetic torque like in the structure from Fig. 6a. By using the H+1 converter with the same control angles it is possible to limit this problem. Moreover, electromagnetic torque ripple are also reduced. By changing supply conditions of the H-type converter, it is possible to obtain the same value of average electromagnetic torque. Simultaneously, it is not possible to get the same level of electromagnetic torque ripple at high-speed as in the H + 1 converter.

6.3. Research results analysis

In Table 1, selected parameters of the motors supplied by H and H + 1 converters were presented. By using the H + 1 converter, it is possible to turn a phase off much later regardless of a rotor profiling type. This allows in a consequence to limit torque ripple and increase average torque T_{eav} (Table 1), because the time period required to discharge accumulated energy in the magnetic field is reduced. The phase current i_{ph} , which flows in a negative slope of an inductance, does not have a tendency to increase when the H + 1 converter is used (Fig. 12, Fig. 17), so in spite of the increase of average electromagnetic torque, its rms value can be decreased (Table 1). Source current ripples are also reduced (Table 1). In structures oriented to a limitation of electromagnetic torque ripple e.g. the analysed structure with a dual step-air gap or the structures presented in [3-4], the impact of the analysed supply method and the control of the two-phase motor is greater. It helps to significantly reduce the ripple of a generated electromagnetic torque of a motor working at a constant power range or on its natural characteristics. In the paper [3], a result of reducing of electromagnetic torque ripple was obtained by using an operation with a constant torque, which causes a decrease of overall efficiency of a drive system. In two-phase structures with a profiled rotor to obtain a small value of a start-up torque (e.g. the analysed structure in Fig. 3a), an increase in an average value of the generated electromagnetic torque with decreased ripple was obtained. Compared to the classic half-bridge converter, voltage requirements of used power electronic elements, (increased number of power electronics elements) and a complexity of a control algorithm also increase.

Table 1. Selected parameters of the motors with an asymmetric magnetic circuit supplied by H and H + 1 converters

Type of an asymmetric magnetic circuit Parameter\circuit	Single step-air gap			Dual step-air gap		
	H	H*	H + 1	H	H*	H+1
Turn-on angle θ_{on} [°]	0	-10	0	0	-2.5	0
Turn-on angle θ_{off} [°]	90	80	90	90	79	90
Average value of electromagnetic torque T_{eav} [N·m]	0.044	0.09	0.09	0.14	0.23	0.23
Maximum value of electromagnetic torque T_{emax} [N·m]	0.26	0.36	0.26	0.53	0.65	0.53
Minimum value of electromagnetic torque T_{emin} [N·m]	-0.16	0.03	0.05	-0.46	0.06	0.13

Electromagnetic torque ripple ε_T [%]	954	333	253	707	261	173
Average value of source current I_{dcav} [A]	0.86	1.56	1.65	2.34	3.74	3.75
Source current ripple ε_I [%]	568	328	258	444	336	224
RMS value of phase current I_{phrms} [A]	2.28	2.42	2.26	4.44	4.28	4.22
Maximum phase voltage u_{phmax} [V]	306	306	649	306	306	564
Minimum phase voltage u_{phmin} [V]	-315	-315	-657	-315	-315	-574

7. Conclusions

The paper presents the results of simulation studies of the modified C-dump converter (marked as H + 1) used to supply high-speed switched reluctance motors. The studies were developed for two structures of two-phase 4/2 switched reluctance motors. The magnetic circuit of the rotor in both structures was profiled to obtain sufficient value of start-up torque in any rotor position. It allows a start-up from each rotor position, but it introduces some limitations in control parameters selection (especially a turn-on angle). It was evident in the structure of Fig. 6b where mechanical characteristic (Fig. 11) was focused on limitation of electromagnetic torque ripple. By using a classic H-type converter, especially at high speed, it is not possible to use a rotor profiling effect, in contrary the C-dump converter (Fig. 5c) gives such an opportunity. By controlling the additional switch S_d , accumulated energy in the magnetic field is discharged faster, so it is possible to turn a winding off much later, which in consequence gives a higher average value of generated electromagnetic torque with the simultaneous decrease of the ripple. Compared to the classic half-bridge converter, voltage requirements of used power electronics elements and a complexity of a control algorithm also increase.

References

- [1] Miller T.J.E., *Switched reluctance motor and their control*, Magna Physics Publishing, Hillsboro, OH and Oxford (1993).
- [2] Krishnan R., *Switched reluctance motor drives: Modeling, simulation, analysis, design, and applications*, CRC Press LLC (2003).
- [3] Dong-Hee L., Huynh K.M.K., Jin-Woo A., *The performance of 2-phase high speed SRM with variable-air rotor poles for blower system*, International Conference on Electrical Machines and Systems (ICEMS), pp. 1595-1598 (2010).
- [4] Tomczewski K., Łukaniszyn M., Witkowski A. et al., *Rotor Shape Optimization of a Switched Reluctance Motor*, Monograph Intelligent Computer Techniques in Applied Electromagnetics, vol. 119, Chapter C, Applications of Computer Methods, Springer, pp. 217-221 (2008).
- [5] Rolim L.G.B., Suemitsu W.I., Watanabe E.H., Hanitsch R., *Development of an improved switched reluctance motor drive using a soft-switching converter*, IEE Proceedings Electrical Power Applications, vol.146, no. 5, pp. 488-494 (1999).
- [6] Tomczewski K., *Power converters extending ranges of operation of switched reluctance motors*, Politechnika Opolska, Studia i Monografie (in Polish), z.321, ISSN 1429-6063, Opole (2012).

- [7] Hava A.M., Blasko V., Lipo T.A., *A modified C-dump converter for variable-reluctance motors*, IEEE Transactions on Industry Applications, vol.23, no. 3., pp. 545-553 (1992).
- [8] Ahn J.W., Liang J., Lee D.H., *Classification and Analysis of Switched Reluctance Converters*, Journal of Electrical Engineering & Technology, vol. 5, No. 4, pp. 571-579 (2010), DOI: 10.5370/JEET.2010.5.4.571.
- [9] Liang J., Lee D.H., Xu G., and Ahn J.W., *Analysis of Passive Boost Power Converter for Three-Phase SR Drive*, IEEE Transactions on Industrial Electronics, vol. 57, no. 9, pp. 2961-2971 (2010), DOI: 10.1109/TIE.2010.2040558.
- [10] Kido Y., Hoshi N., Chiba A., Ogasawara S., Takemoto M., *Novel Switched Reluctance Motor Drive Circuit with Voltage Boost Function without Additional Reactor*, Proceedings of the 2011-14th European Conference on Power Electronics and Applications (EPE 2011), Brimingham, United Kindom, pp. 1-10 (2011).
- [11] Tomczewski K., Wrobel K., *Improved C-dump converter for switched reluctance motor drives*, IET Power Electronics, vol. 7, no. 10, pp. 2628-2635 (2014), DOI: 10.1049/iet-pel.2013.0738.
- [12] Teodosescu P.D., Rusu T., Martis C.S., Pop A.C., Vintiloiu A.C., *Considering Half Bridge Converters for Switched Reluctance Motor Drive Applications*, 2015 Intl Aegean Conference on Electrical Machines & Power Electronics (ACEMP), 2015 Intl Conference on Optimization of Electrical & Electronic Equipment (OPTIM) & 2015 Intl Symposium on Advanced Electromechanical Motion Systems (ELECTROMOTION) Side, Turkey, pp. 186-191 (2015), DOI: 10.1109/OPTIM.2015.7427021.
- [13] Deriszadeh A., Adib E., Farzanehfard H., Nejad S.M.S., *Switched reluctance motor drive converter operating in continuous conduction mode with high demagnetisation voltage*, IET Power Electronics, vol. 8, no. 7, pp. 1119-1127 (2015), DOI: 10.1049/iet-pel.2014.0788.
- [14] Yi F., and Cai W., *A Quasi-Z-source Integrated Multiport Power Converter as Switched Reluctance Motor Drives for Capacitance Reduction and Wide-Speed-Range Operation*, IEEE Transactions on Power Electronics, vol. PP, no. 99, pp. 1-1 (2016), DOI 10.1109/TPEL.2016.2521351.
- [15] Lee D.H., Lee J., Ahn J.W., *Current control of a high speed SRM with an advanced 4-level converter*, 2011 IEEE 8th International Conference on Power Electronics and ECCE Asia (ICPE & ECCE), Jeju, Korea, pp. 109-114 (2011), DOI: 10.1109/ICPE.2011.5944558.
- [16] Tomczewski K., Wrobel K., *Quasi-three-level converter for switched reluctance motor drives reducing current rising and falling times*, IET Power Electron., vol. 5, no. 7, pp. 1049-1057 (2012).
- [17] Bogusz P., Korkosz M., Prokop J., Powrózek A., *A Two-phase Switched Reluctance Motor with Reduced Stator Pole-arc*, 18th International Conference on Electrical Drives and Power Electronics, EDPE 2015, Tatranska Lomnica, Slovakia, pp. 312-318 (2015), DOI: 10.1109/EDPE.2015.7325312.
- [18] Bogusz P., Korkosz M., Prokop J., *Modified method of supply and control of switched reluctance motor*, LI International Symposium on Electrical Machines, Zeszyty Problemowe – Maszyny Elektryczne, Nr3/2015(z.107) (in Polish), Chmielno, Poland, pp. 51-56 (2015).
- [19] The MathWorks Inc., *Matlab Documentation* (2012).
- [20] Prokop J., *Mathematical modeling of switched electric machines*, Oficyna Wydawnicza Politechniki Rzeszowskiej (in Polish), ISBN 978-83-7199-867-8, Rzeszow (2013).